Published in final edited form as:
J Comp Neurol. 2010 July 15; 518(14): 2841–2853. doi:10.1002/cne.22367.

Role of transverse bands in maintaining paranodal structure and axolemmal domain organization in myelinated nerve fibers: effect on longevity in dysmyelinated mutant mice

Amanda J. Mierzwa[1], **Juan-Carlos Arevalo**[3], **Rolf Schiff**[2], **Moses V. Chao**[3,4], and **Jack Rosenbluth**[1,2]

[1] Department of Physiology & Neuroscience, New York University School of Medicine, New York, New York

[2] Rusk Institute, New York University School of Medicine, New York, New York

[3] Skirball Institute of Biomolecular Medicine, New York University School of Medicine, New York, New York

[4] Molecular Neurobiology Program, New York University School of Medicine, New York, New York

Abstract

The consequences of dysmyelination are poorly understood and vary widely in severity. The ‘shaking’ mouse, a quaking allele, is characterized by severe CNS dysmyelination and demyelination, a conspicuous action tremor and seizures in ~25% of animals, but with normal muscle strength and a normal lifespan. In this study we compare this mutant with other dysmyelinated mutants including the ceramide sulfotransferase deficient (CST−/−) mouse, that are more severely affected behaviorally, to determine what might underlie the differences between them with respect to behavior and longevity. Examination of the paranodal junctional region of CNS myelinated fibers shows that ‘transverse bands’, a component of the junction, are present in nearly all ‘shaking’ paranodes but in only a minority of CST−/− paranodes. The number of terminal loops that have transverse bands within a paranode and the number of transverse bands per unit length are only moderately reduced in the ‘shaking’ mutant, compared with controls, but markedly reduced in CST−/−. Immunofluorescence studies show also that although the nodes of the ‘shaking’ mutant are somewhat longer than normal, Na^+ and K^+ channels remain separated, distinguishing this mutant from CST−/− and others that lack transverse bands. We conclude that the essential difference between the ‘shaking’ mutant and others more severely affected is the presence of transverse bands, which serve to stabilize paranodal structure over time as well as the organization of the axolemmal domains, and that differences in the prevalence of transverse bands underlie the marked differences in progressive neurological impairment and longevity among dysmyelinated mouse mutants.

Keywords

axon degeneration; demyelination; multiple sclerosis; quaking; glycolipid

Corresponding author and address: Dr. J. Rosenbluth, Department of Physiology and Neuroscience, NYU School of Medicine, 550 First Avenue, New York, NY 10016, rosenj03@med.nyu.edu.

INTRODUCTION

During development, the axon and the oligodendrocyte communicate and establish distinct axoglial domains, distinguished by structural features (Rosenbluth, 1995a) as well as their ion channel and protein composition (Sherman and Brophy, 2005). Their formation and maintenance seem to be essential for the proper function of the axon—the propagation of the action potential. The paranode is a highly structured domain where individual myelin lamellae attach to the axon as cytoplasm-containing 'terminal loops'. In aldehyde-fixed specimens, these junctions, which are similar to invertebrate septate junctions (Baumgartner et al., 1996). are characterized by intercellular 'transverse bands'(TBs). The proposed functions of the TBs include anchoring the paranodal loops to the axon, minimizing the periaxonal space to prevent current loss, and maintaining the distinct axonal domains (Rosenbluth, 1995a; 2009).

'Myelin mutants' such as the Caspr −/− (Bhat et al., 2001), contactin −/−(Boyle et al., 2001), and ceramide galactosyltransferase deficient (CGT−/−) mice (Dupree et al., 1998) lack TBs completely. Their paranodes show many defects in the attachment of the paranodal loops to the axon, and the space between the loops and axon may be increased (Boyle et al., 2001). Loops may be completely detached and even everted, facing away from the axon. All of these animals have shortened lifespans and severe neurological defects including tremor, seizures, hypomotility, and paresis. The paranodes in other 'myelin mutants' such as the ceramide sulfotransferase deficient (CST−/−) mouse (Marcus et al., 2006) and in cultured CNS from DCC−/− or Netrin-1−/− mouse pups (Jarjour et al., 2008) develop TBs in a normal fashion, but the TBs largely disappear and the paranodes progressively deteriorate as the mice mature.

The spontaneously occurring 'shaking' mutant (Mierzwa et al., 2004) described in this paper has many similarities to other myelin mutants. There is a gross deficit in CNS myelin, and the animals have an action tremor appearing ~P12. Despite significant morphological abnormalities in CNS myelin, this mutant has no apparent muscle weakness or paresis, and the lifespan is normal. It is unclear why this mutant, with equal or greater dysmyelination in comparison with mutants such as the CST−/−, does not have equally severe neurological defects or a shortened lifespan.

We have examined the paranodes of three groups of animals, control, 'shaking', and CST−/−, to determine whether the absence/presence of TBs is related to the degree of neurological deficit and ultimately the lifespan of the animal.

METHODS

Animals

All animal procedures were carried out in accordance with our protocols #050713 and 081007 approved by the NYU School of Medicine Institutional Animal Care and Use Committee.

Breeding

'Shaking'—The mutation is carried in an autosomal recessive manner in mice of mixed genetic background (C57BL/6 – 129/Sv). Breeding was carried out between a heterozygote and a homozygous recessive mutant resulting in 50% of pups affected. Both sexes of homozygous recessive animals are capable of breeding. Mutant animals were identified ~P12 by the presence of an action tremor. Littermates (heterozygotes) were used as controls.

To determine whether 'shaking' is an allele of quaking we also bred a homozygous 'shaking' female mouse with a heterozygous quaking male mouse (Jackson Laboratories, stock number 005089) and analyzed the behavior of the pups in the three litters obtained.

CST−/−—CST −/− were bred through heterozygote X heterozygote matings. All animals were genotyped by PCR as described in Honke et al. (2002).

Histology and Electron Microscopy

Anesthetized animals were fixed by cardiac perfusion with 3% glutaraldehyde/2% formaldehyde in 0.1M cacodylate buffer (pH ~7.3). The spinal cord was dissected and slices were post-fixed in 2% osmium tetroxide in 0.1M cacodylate buffer. Slices of cervical spinal cord were subsequently dehydrated in a graded methanol series, left overnight in propylene oxide, and embedded in Araldite. Thick sections (~1μ) were cut and stained with toluidine blue to be viewed, using a 40X or 100X objective (N.A. 1.3), and photographed with a digital camera (Nikon CoolPix990). Thin sections (~0.1μ) were cut and stained with $KMnO_4$ and uranyl acetate and viewed with an electron microscope (JEOL JEM-1200 EX II at 80kV, JEOL JEM-100CX at 60kV or Philips EM300 at 60 kV). Micrographs were taken at 3K, 10K or 25K magnification.

Behavioral analysis

Animals were observed approximately once a week in their cages. Cages were moved to check for motion-induced seizures. If witnessed, the approximate duration and type of seizure was noted. Prior to fixation, animals were lifted by their tails to check for hindlimb clasping. In addition, animals were placed on the edge of a metal cage lid which was tilted so the animal had to support itself with its front limbs. The ability to hang for at least 15s was considered successful.

Rotarod testing was performed using 4-month control and 'shaking' male mice following a two day protocol. Day one consisted of three training trials of five minutes each separated by at least 15 minutes. If the animal fell off the wheel, it was placed back on until five minutes expired. On day two, animals completed three five-minute trials separated by at least 15 minutes. Animals were allowed to walk for five minutes or until they fell from the wheel. All trials were videotaped to allow for accurate timing of trials.

To examine the gait of control and 'shaking' animals the paws of each animal were painted (front and back paws in different colors) with non-toxic paint. The animal was placed at the beginning of a paper-lined cardboard tunnel and allowed to walk back to its cage. The distance between footprints was measured and abnormalities in the gait were also documented.

Immunofluorescence

Animals were anesthetized and fixed by cardiac perfusion with 1 or 2% paraformaldehyde. After 30 minutes, the spinal cord was dissected and rinsed in Ringer's overnight. Spinal cord segments were cut and soaked overnight in 30% sucrose. Segments of spinal cord were cut into 20–40μ sections using a cryostat, collected in Ringer's, dried on subbed slides, and stored at −20°C until used.

Thawed slides were blocked with 10% donkey or goat serum and 0.1% Triton X-100 in 0.1M phosphate buffer for a minimum of three hours. Primary antibody, diluted as described in Table 1 in either blocking solution, was left on overnight. Primary antibodies include αpanNa (Sigma), αCaspr (courtesy of Dr. E. Peles, The Weizmann Institute of Science, Israel), and αKv1.2 (Alamone Labs and K14/16; Neuromab; www.neuromab.org). After

rinsing (3×10min, 0.1M phosphate buffer), secondary antibody, coupled to a fluorophore (Texas red or FITC), was applied for one hour and rinsed (3×10min, 0.1M phosphate buffer). Secondary antibodies were purchased from Jackson ImmunoResearch. The sections were covered with Vectashield anti-fade mounting medium and imaged using a confocal microscope.

The confocal mages were recorded in black and white, then assigned colors (green for fluorescein and red for Texas red) in ImageJ (NIH). Adobe Photoshop was used to adjust brightness and contrast, and the clone stamp tool was used to remove extraneous fluorescent elements from the background

All measurements were performed using ImageJ software. Further details of antibodies are given in Table 1.

Data analysis

To determine g-ratio, electron micrographs were digitized. In order to compensate for irregularities in fiber shape, ImageJ software was used to trace the circumference of each axon and the circumference of the fiber (axon + myelin). The ratio of the respective circumferences is equivalent to axon diameter/fiber diameter = g ratio.

Images of longitudinally sectioned paranodes, both printed and digitized, were examined and scored in a blind fashion. To determine the percentage of loops with TBs, the number of loops with TBs was counted and divided by the total number of loops contacting the axon in each paranode. The number of TBs per unit length was determined also using ImageJ. All length measurements were made along glial membranes of paranodal loops up to the junctions with the immediately adjacent loops. Only loops that had at least one TB present and a periaxonal cleft bordered by clear membranes were used. The adjusted # TBs/micron was calculated as # TBs/micron X % loops with TBs/100 using the values from the previously described counts.

Statistical analyses

Results were tabulated using Microsoft Excel and statistics were determined using SPSS 13.0. A t-test was used to evaluate the differences between two population means. A z-test was used to evaluate the differences between two population proportions. Standard deviations and confidence levels are reported as appropriate.

Immunoblot analysis

Brain lysates were obtained using lysis buffer containing 20 mM Tris-HCl pH 8, 137 mM NaCl, 1% NP-40, 0.2% SDS, 2 mM EDTA and protease inhibitors (0.15 units/ml of aprotinin, 20 μM leupeptin and 1 mM phenylmethylsulphonylfluoride). Protein concentration was assessed and equal amounts were analysed by SDS-PAGE followed by western blot using different antibodies. Reactive protein bands were visualized by enhanced chemiluminiscence detection (Amersham Corp.). The authors thank Drs. E. Peles and J. Salzer for providing antibodies used in the immunoblot analysis. Further details of antibodies are given in Table 1.

Antibody characterization

Table 1 lists the antibodies used for immunofluorescence and western blots.

MBP antibody recognized 4 isoforms, 21.5, 20.2, 18.5, and 17.2 kD from mouse brain similar to the ones reported by Graziano et al. (2008).

CNPase antibody recognized both CNP1 (46kD) and CNP2 (48kD) bands on western blots of mouse brain as previously described (Miotke et al., 2007).

CnFc antibody recognized only a specific band of 150 kD as previously reported by Yoshihara et al., 1994.

Caspr antiserum recognized only a single band (190 kD) on western blots of mouse brain in a similar fashion as previous reports (Peles et al., 1997). IHC shows specific staining of rat optic nerve paranodes by this antibody (Poliak et al., 1999).

Actin antibody recognized only a single band of 42 kD on western blots according to the manufacturer's datasheet. In our hands, a single band of 42 kD was observed from mouse brain lysates.

PanNav antibody reacts strongly with with Na+ channels in mammalian central and peripheral nervous system, as stated by the manufacturer. IHC showed staining of nodes of Ranvier in normal rat optic nerve, as previously described (Rasband et al., 1999).

Kv1.2 antibody from Alomone Labs detected a single band not present when the antibody was preincubated with the antigen, as stated by the manufacturer. IHC showed staining of the juxtaparanodal region in normal optic and sciatic nerves of mice (Rios et al., 2003).

Kv1.2 antibody from Neuromab has been previously characterized in immunoblots from rat brain membrane extracts by Bekele-Arcuri et al., (1996) and shown to stain the juxta-paranodal region of myelinated axons in normal rat subcortical white matter.

RESULTS

Breeding

'Shaking' mice display abnormalities in the CNS and to a lesser extent in the PNS (Mierzwa et al., 2004), resembling in this respect the quaking mouse mutation (Rosenbluth, 1995b; Samorajski et al., 1970; Suzuki and Zagoren, 1977). In order to determine whether the respective mutants are alleles, we cross bred them. Specifically, a homozygous 'shaking' mouse female was mated with a heterozygous quaking male. If they are in fact alleles, ~50% of the offspring should exhibit the characteristic action tremor.

Three litters of animals were obtained. In the first, one of three pups displayed the tremor. In the second, a litter of five born three months later, one pup died before its phenotype could be determined, and two of the remaining four displayed the tremor. In the third litter, born two months later, two of four pups displayed the tremor. Overall, five of eleven pups from the 'shaking' quaking cross were affected. The simplest explanation is that the 'shaking' mutation is a quaking allele. Indeed, positional cloning studies have localized the gene to a 9.3 Cm region (7.1 to 16.4) of chromosome 17 that includes the qk locus. Nevertheless, it remains possible that more complex explanations such as haploinsufficiency at multiple loci could account for our data. To definitively answer this question, further mapping of the 'shaking' mutation is needed. This work is in progress.

Behavior

The 'shaking' mutant is a spontaneously occurring mutation which was first identified by an action tremor apparent ~12 days after birth (Mierzwa et al., 2004). Tonic seizures are witnessed in ~25% of animals starting after six weeks and lasting throughout adulthood. These seizures are typically motion-induced, occurring when the cage is moved or may be

induced by twirling the animal by the tail. They typically last 30–60 seconds without cessation of breathing.

Animals remain motile throughout their lives with no evidence of paresis. However, the stride of 'shaking' animals is shorter than control and lacks a regular pattern of paw positioning. Rotarod testing of control and 'shaking' animals revealed no difference in the ability of the 'shaking' mice to remain on a moving surface (walking latency: control=198s, 'shaking'=223s; n.s.) (Mierzwa et al., 2005). Interestingly, many 'shaking' animals grip the walking surface and 'ride' the Rotarod around. Apparently these mice are unable to keep up with the speed of walking required to stay atop the walking surface. This aberrant behavior does, however, demonstrate muscle strength, as all limbs are able cling to the Rotarod while the animal is upside down. Further tests of muscle strength show that all animals tested, regardless of age, are able to hang from front or hind limbs from the edge of a cage. There does not appear to be a progression in the neurological signs and animals can survive to at least two years without any special care.

Histology and electron microscopy

Light microscopy of the dorsal columns in 'shaking' cervical spinal cord shows decreased numbers of myelinated axons and thinner myelin at all ages examined (3wks-2yrs) (Fig. 1B) in comparison with control (Fig. 1A) or CST−/− (Fig. 1C) dorsal columns. Electron microscopy of 'shaking' spinal cord or optic nerve (Fig. 1D) shows large numbers of thinly myelinated and unmyelinated axons of a caliber that would normally be myelinated. (See Marcus et al. (2006) for illustrations of normal and CST−/− CNS myelin.) A sample of 'shaking' optic nerve showed that 317 of 455 axons (~70%) were unmyelinated. In the dorsal columns, average g-ratio measurements show that myelin in the 'shaking' animal is significantly thinner than that in control animals (control = 0.83 vs 'shaking' = 0.91, $p<0.001$) (Table 2). In addition, there are several other abnormalities including redundant myelin and cytoplasm-containing myelin lamellae (Fig. 1D), heminodes, elongated nodes, and abnormal paranodes. In contrast, the 'shaking' PNS is almost fully myelinated. Paranodal abnormalities are similar but occur to a lesser degree (not illustrated).

Paranodal structure

The dorsal columns of cervical spinal cords in control, 'shaking', and CST−/− animals were photographed to show paranodal detail. Figure 2 highlights the structural features of normal and abnormal paranodes. The great majority of paranodal loops in the control and 'shaking' animals contact the axon. This junction is characterized by a 'scalloping' of the axolemma where individual loops indent the axon. There are loops which do not contact the axon, but the majority of these end on other paranodal loops. A few everted loops (control 11%, 'shaking' 7%) face away from the axon (Table 3). Interestingly, the 'radial component' (RC) is prominent in the paranodal region of the 'shaking' mutant (Fig. 3D). This differs from control paranodes where the RC is rarely seen. It is possible that the enhanced RC serves to tether loops that have separated from the axon to the remainder of the paranode and prevents them from retracting (Gow et al., 1999).

The paranodes in CST−/− animals are not quantitatively different in the number of loops that contact the axon, but qualitatively the paranodes are different. There is not a difference in the number of everted or detached loops compared to control (Table 3), but the detached loops that do not meet the axon are rarely wedged between other loops as in the control or 'shaking' animals. Rather, these non-contacting loops tend to be adjacent to the node and pulled away from it (Fig. 2). In some cases, a loop near the juxtaparanode will undercut other loops closer to the node so that the other loops terminate on the innermost paranodal loop rather than the axon, thus preventing all remaining paranodal loops from contacting the

axon. This has been reported in the 'shaking' animal as well (Mierzwa et al., 2004), and comparable 'stripping' of paranodal myelin loops from the axon by an astrocyte process has been reported in the Caspr−/− mutant (Bhat et al., 2001).

In addition to the paranodes we scored, there were many paranode-like structures seen in the CST−/−. These are distinct from true paranodes because they are not adjacent to a node and are often found under or within layers of compact myelin lamellae. In addition, 'pseudonodes', sets of loops coming from both sides that are not separated by a gap and are covered by compact lamellae, are seen. The way in which these structures are formed is unclear, but as they do not form next to a node, we do not consider them to be paranodes.

Transverse bands

In control animals, there are regular, densely stained TBs in the cleft between the paranodal loop and axon (Fig. 3A). TBs are found throughout the paranodal junction spanning the cleft from the juxtaparanode to the node in 100% of paranodes examined. The vast majority of 'shaking' paranodes (94%) also have TBs (Fig. 3B, C). However, only a small portion of CST−/− paranodes have TBs (Table 3). It was reported that the CST−/− has limited numbers of TBs, which are more prevalent at early ages and seem to disappear as the animals age (Marcus et al., 2006). We find that TBs are present in ~16% of paranodes across age groups (1.5mo to 12mo), significantly less than the proportion seen in control or 'shaking' (both $p<0.001$).

Despite the fact that TBs are present in the majority of 'shaking' paranodes, TBs do not appear as commonly as they do in control animals (Table 4). Often the spacing between TBs is irregular, or paranodal loops or portions of loops lack well-defined TBs. Scoring individual paranodal loops (excluding those that are everted or removed from the axon), significantly more loops in control animals have at least one TB than in the 'shaking' animal (91% versus 62%, $p<0.001$; Table 4). In addition, those loops in the 'shaking' animal that have TBs have fewer per loop. Using only those paranodal loops that had at least one TB, the number of TBs on each loop was counted and the length of the loop measured. Normalizing to a length of one micron, in those loops that have TBs, there are modestly more TBs per micron of junctional loop membrane in the control animal (control=23.2 ± 3.4 vs 'shaking'=20.2 ± 6.7, $p=0.04$). To include *all* loops, both with and without TBs, we calculated an adjusted number of TBs per micron of junctional loop membrane (Table 4). In that case, the number of TBs per micron in the 'shaking' mice is ~59% of that of control ('shaking' 12.5 vs control 21.1).

Protein levels

Transverse bands are reduced by about half per paranode, as described above. In addition, the proportion of axons that are myelinated is also markedly reduced, probably by more than half, based on the data presented above. Thus, transverse bands as a function of total axonal volume would be even further reduced in comparison with control CNS. This raises the possibility that the axonal PNJ components Caspr and contactin might be reduced proportionately. Alternatively these elements might be present at normal levels but distributed differently, i.e., not localized to axonal paranodes.

Accordingly, we compared western blots of Caspr and contactin (CnFc) in the CNS of shaking and control mice in order to assess levels of these proteins at various ages. As Fig. 4 shows, both proteins are present at approximately normal levels at all ages examined. This is in marked contrast to the levels of CNPase and MBP, components of compact myelin, that are clearly reduced, presumably reflecting the quantitative diminution in compact myelin in

the shaking mice. These results correspond to those obtained in studies of other mutants deficient in transverse bands (Ishibashi et al. 2002;Pillai et al. 2009).

Channel Segregation

Since TBs are present in the 'shaking' animal, we wondered whether the voltage-gated Na^+ and K^+ channels are normally segregated. To test this we looked at longitudinal spinal cord sections from adult animals 6–7.5 months old. Nodal and paranodal lengths were measured on sections double stained with αpanNa and αCaspr. The Caspr localization we found was comparable to that shown in Poliak et al., (1999). At 7.5mo, shaking nodes were ~37% longer than control nodes (control=0.65μ vs shaking=0.89μ, p=0.003). The length of paranode stained was somewhat variable (Fig. 5A, B), but on average there was no significant difference in the length of paranodes (control=1.99μ vs 'shaking' 2.08μ, ns; Table 2). Double staining with αpanNa and $\alpha K_v1.2$ shows clear separation of these channels (Fig. 5C,D) comparable to that seen in previous studies (Bekele-Arcuri et al., 1996; Rasband et al, 1999; Rios et al., 2003). Again, the length of $\alpha K_v1.2$ staining was variable but a clear separation from αpanNa staining was present in all fibers examined.

Comparable immunostains of shaking sciatic nerve also showed clear separation of nodal sodium channel from juxtaparanodal potassium channel domains. Measurement of shaking PNS node length showed it to be increased by ~18% (control=0.75μ vs shaking 0.89μ, p= 0.019). PNS paranode length showed no significant difference from control (data not shown).

DISCUSSION

Summary

Our major findings are: TBs were found in all control paranodes and nearly all 'shaking' paranodes. However, consistent with previous reports (Marcus et al., 2006), TBs were present in only a minority of CST−/− paranodes. In control animals, over 90% of paranodal loops had at least one TB compared to 62% of paranodal loops in 'shaking' mice. The number of TBs per unit length of junctional glial membrane in 'shaking' paranodes is ~59% that in controls. Ion channel domains are localized normally in the 'shaking' mice, with Na^+ channels at the node separated by a normal length paranode from $K_v1.2$ channels at the juxtaparanode. Finally, the compact myelin proteins MBP and CNPase are reduced at all ages in shaking mouse brain. Caspr and contactin are present at normal levels.

Mutants lacking transverse bands

A number of mutants have been engineered that knock out the paranodal proteins Caspr (Bhat et al., 2001), contactin (Boyle et al., 2001), or neurofacin 155 (NF155) (Pillai et al., 2009) or that knock out an enzyme responsible for making a component of the myelin lipid rafts, e.g., CGT (Dupree et al., 1998). Examination shows myelin forming normally, but TBs completely absent. Many paranodal abnormalities occur including everted loops, paranodal loops abutting or overlying loops from the opposite side, and astrocyte processes extending between the myelin and axolemma. Channel segregation is incomplete. Voltage-gated K^+ channels, normally concentrated in the juxtaparanode, are found in the paranodal region close to nodal Na^+ channels. The lack of TBs seems to underlie the inability to maintain normal paranodal structure and axoglial domains.

The neurological defects in animals completely lacking TBs are severe. These animals develop neurological signs by two weeks after birth including tremor, motor paresis, and ataxia. The NF155−/− (Pillai et al., 2009) and contactin −/− (Boyle et al., 2001) mutants live only to postnatal day 18. Most Caspr −/− pups die around the time of weaning, although

with special care they can live at least five months (Bhat et al., 2001). It is apparent that without TBs, mutant animals lose motor functions and do not live long into adulthood

Transverse bands are not required for the initial differentiation of the axolemma.into nodal, paranodal and juxtaparanodal domains (Rosenbluth et al 2003; Marcus et al. 2006). However, in mutants characterized by the absence of TBs, axonal differentiation is not maintained.. Paranodes undergo remodeling over time resulting in gradual changes in the size and shape of the nodal domain. The ultimate result is grossly misshapen nodes that may be greatly elongated and that may be only partially occupied by voltage-gated sodium channels (Rosenbluth et al., 2003). Thus, one of the primary functions of TBs is to maintain the attachment of the myelin sheath to the paranodal axon over time, presumably by interlinking axonal and glial cytoskeletal elements, and thus stabilize the form of the axolemmal domains, in particular the size of the node, as well as maintain separation of nodal sodium channels from juxtaparanodal potassium channels.

The consequences of nodal enlargement in mutants lacking TBs can be profound (Rosenbluth, 2009). As nodal area enlarges, nodal capacitance would increase and nodal transmembrane resistance decrease. Nodal sodium channels may become ‘diluted’. Ultimately as these changes progress, passive depolarization of the node would become insufficient to generate action potentials. These events in even a small number of nodes in the chain along an axon would be sufficient to block saltatory conduction in that axon. Over time, conduction failure in a gradually increasing proportion of the myelinated axons comprising a fiber tract would lead to a gradual decline in the functions mediated by that tract. The result, in the motor system, would be progressive decline in motor abilities to the point that vital functions such as eating, drinking and breathing became increasingly compromised, leading to the death of the animal. In short, stability of the paranodal junction is needed for maintaining constancy of nodal size and electrical parameters in myelinated fibers, and these in turn are required for reliable signal propagation. Paradoxically, in the complete absence of myelin, ion channels are uniformly distributed, and axons can propagate signals by slow continuous conduction; i.e. defective myelin can be worse than none.

The possibility that cytoskeletal interlinkage in the paranodal region once established may persist even after loss of transverse bands has been suggested based on analysis of a conditional knockout of NF155. Following selective ablation of NF155 at P23, TBs progressively disappeared from the paranodal junction, associated with ‘near-complete’ loss of NF155 but nevertheless ‘near-normal’ conduction (Pillai et al. 2009). The lifespan of these animals was not reported. These observations raise the interesting alternative possibility that even small amounts of NF155 remaining in the knockdown may be sufficient to form enough TBs to preserve paranodal junctional integrity well enough to maintain axonal conduction, at least temporarily. Such appears to be the case in the CST−/− mouse, which has a markedly reduced number of TBs but is able to survive as long as 15mo (Marcus et al., 2006).

Mutants with reduced numbers of transverse bands

The quaking viable mouse (qk^v) was first described as having an action tremor at the onset of myelination, weak hindlimbs, seizures beginning at three months, and a lifespan of “at least several months” (Sidman et al., 1964). TBs were seen only rarely in the PNS (Suzuki and Zagoren, 1977). It is unclear at what frequency TBs appear in the qk^v CNS. However, some of the axonal paracrystallinity characteristic of the paranodal junction is visible in freeze-fracture replicas (Rosenbluth, (1995b)

More is known about the CST −/− mouse where paranodal deterioration is mirrored by an increasing level of dysfunction (Ishibashi et al., 2002). Young animals form relatively normal myelin with established node and paranode regions (Marcus et al., 2006). Prior to one month, the only behavioral defect is a tremor. After one month, nodal structure breaks down and evidence of myelin degeneration is present (Marcus et al., 2006). Our data show that by 1.5 months of age, the earliest point we examined, many of the TBs have disappeared, and only a minority of paranodes display TBs. Slow breakdown of paranodes may underlie a slowly progressive conduction block (Rosenbluth, 2009). This occurs first in the longest axons as evidenced by weakness in the lower limbs and eventually moves rostrally. In addition, large caliber axons degenerate by 8 months (Marcus et al., 2006). At about the same time, we see an inability of the animals to properly right themselves, and hypomotility. By 8–9 months animals primarily lie on their sides in the cage. The lifespan in these animals is significantly longer than that in the animals completely lacking TBs. However, animals never live past 15 months.

Thus, the presence of some TBs and normal paranodes seems to prolong function and improve survival in these animals. Previous studies of the PNS in CST−/− mice shows mislocation of Kv channels to the paranode, but otherwise PNS myelinated fibers are relatively normal in appearance at all ages examined in contrast to CNS fibers which deteriorate over time. Thus, it is likely that the progressive neurological deficits in these mice and their shortened lifespan are the result of the CNS pathology.

A similar phenotype is seen in β1,4-*N*-acetylgalactosaminyltransferase (GalNAc-T) knockout mice, which lack complex gangliosides leading to altered lipid rafts (Susuki et al., 2007). Paranodes form normally but maintenance is affected and paranodal abnormalities increase with age. TBs are found in some but not all paranodal loops. Kv1 channel staining overlaps with Caspr and NF155 immunoreactivity, and Nav nodal staining is longer, showing that without a full complement of TBs ion channels may shift. Slowly progressive neurological defects occur, similar to those in CST−/− mice, and animals survive up to 14 months.

Mutants with mislocalized transverse bands

TBs seem to be needed to maintain paranodal junction structure, but they alone cannot maintain function. They must secure myelin to the axon in well organized paranodes. TBs are found in the paranodes of the shiverer mouse, although not as consistently as in normal animals (Rosenbluth, 1980; 1981). However, TBs are also found at abnormal myelin formations between glial processes and the axolemma in regions that are not clearly paranodal. There may be multiple glial processes forming junctions with the axolemma in different orientations held in place with TBs. The end result is an abundance of aberrant axoglial junctions with TBs that are not associated with nodes. These animals have a tremor starting at the onset of myelination and tonic seizures which increase in severity and duration. Most animals die within 4 months (Jacobs, 2005). Thus, it isn't enough to just secure glial processes to the axon. Separation of the ion channels into distinct Na^+ channel-containing nodal domains and separate juxtaparanodal K^+ channel domains appears to be necessary.

Mutants with many transverse bands

TBs are found in many paranodes in the MAL−/− mouse (Schaeren-Wiemers et al., 2004). This mutation affects only the CNS where myelination is delayed and there are abnormal cytoplasmic inclusions in compact myelin. Like the 'shaking' animal, this animal has a normal lifespan. Although TBs are present, they are reported to be not as "organized" as in the control animal. They are absent from some paranodal loops and may appear as "diffuse

electron-dense areas" rather than discrete densities. Yet, separation of the nodal Na^+ and juxtaparanodal K^+ channels is maintained. As in the 'shaking' mutant, TBs are present and lifespan is normal.

There are many unmyelinated axons in the 'shaking' animal. However, there seem to be enough that are myelinated and have those structures found in "normal" paranodes including TBs to prevent debilitating motor paresis. Evidently, the presence of TBs in the 'shaking' animal helps maintain paranodal structure and maintain nodes at a rather constant, albeit longer, length than normal. Even with a reduced frequency of TBs, the separation of the nodal Na^+ channels and the juxtaparanodal K^+ channels is maintained in these animals. The fact that TBs are not as regular or as frequent as in normal animals opens up the possibility that the junction may be "leakier" than normal. This plus increased nodal length, and thinner myelin may contribute to slowed conduction in the 'shaking' mutant (Mierzwa et al., 2008). The animals maintain motility and muscle strength throughout their lives and routinely live to at least two years. It is likely that the presence of TBs in nearly all paranodes and the role they play in maintaining axoglial domains maintains function in 'shaking' myelinated fibers.

Functions of transverse bands

TBs are needed to maintain the paranodal junction. While the junction can form without TBs, the junction is not stable and progressively breaks down. Various myelin mutants have been engineered that lack TBs including the CGT −/− (Dupree et al., 1998), the Caspr −/− (Bhat et al., 2001), the contactin −/− (Boyle et al., 2001), and the NF155 −/−(Pillai et al., 2009). In these mutants, many paranodal loops appear detached from the axon with everted loops in those lamellae closest to the node. Potassium channels are not segregated to the juxtaparanode, but are found in the paranode and up to the sodium channels in the nodal domain. Without ties to the axon, myelin shifts and retracts from the axon leaving large areas of exposed axon comparable to the greatly elongated nodes seen in the CGT−/− CNS (Rosenbluth et al., 2003). Eventually, as outlined above, in 'Mutants lacking transverse bands', the distorted nodal structure can no longer support saltatory conduction, leading to conduction block that underlies the worsening neurological defects and ultimately death.

Conclusions

'Shaking' animals have a severe deficit in the overall amount of myelin and are similar in that respect to other 'myelin mutants', e.g. the CST −/− or CGT−/−. In 'shaking' animals, however, the neurological consequences are modest and lifespan is normal. Despite their superficial similarities, these mutants clearly differ in that TBs are present in the 'shaking' mice to a much greater degree. In view of this correlation, we suggest that TBs underlie the longevity of 'shaking' mice by maintaining the structure of the paranodal junction, thereby preserving the axolemmal domain organization and constancy of nodal dimensions required for reliable saltatory conduction.

Supplementary Material

Refer to Web version on PubMed Central for supplementary material.

Acknowledgments

Support: This work was supported by grants NS037475 (JR) and NS051282 (MC) from the NIH and grant RG 3618 (JR) from the National Multiple Sclerosis Society.

The authors would like to thank Dr. Seema Shroff for reviewing the manuscript, Dr. Eric Lang for helpful discussions and Chris Petzold for expert technical assistance. A preliminary report of this study was presented at a Society for Neuroscience meeting (Rosenbluth et al., 2008).

References

Baumgartner S, Littleton JT, Broadie K, Bhat MA, Harbecke R, Lengyel JA, Chiquet-Ehrismann R, Prokop A, Bellen HJ. A Drosophila neurexin is required for septate junction and blood-nerve barrier formation and function. Cell. 1996; 87(6):1059–1068. [PubMed: 8978610]

Bekele-Arcuri Z, Matos MF, Manganas L, Strassle BW, Monaghan MM, Rhodes KJ, Trimmer JS. Generation and characterization of subtype-specific monoclonal antibodies to K+ channel alpha- and beta-subunit polypeptides. Neuropharmacology. 1996; 35:851–65. [PubMed: 8938716]

Bhat MA, Rios JC, Lu Y, Garcia-Fresco GP, Ching W, St Martin M, Li J, Einheber S, Chesler M, Rosenbluth J, Salzer JL, Bellen HJ. Axon-glia interactions and the domain organization of myelinated axons requires neurexin IV/Caspr/Paranodin. Neuron. 2001; 30(2):369–383. [PubMed: 11395000]

Boyle ME, Berglund EO, Murai KK, Weber L, Peles E, Ranscht B. Contactin orchestrates assembly of the septate-like junctions at the paranode in myelinated peripheral nerve. Neuron. 2001; 30(2):385–397. [PubMed: 11395001]

Dupree JL, Coetzee T, Blight A, Suzuki K, Popko B. Myelin galactolipids are essential for proper node of Ranvier formation in the CNS. J Neurosci. 1998; 18(5):1642–1649. [PubMed: 9464989]

Garcia-Fresco GP, Sousa AD, Pillai AM, Moy SS, Crawley JN, Tessarollo L, Dupree JL, Bhat MA. Disruption of axoglial junctions causes cytoskeletal disorganization and degeneration of Purkinje neuron axons. Proc Natl Acad Sci USA. 2006; 103:5137–5142. [PubMed: 16551741]

Gow A, Southwood CM, Li JS, Pariali M, Riordan GP, Brodie SE, Danias J, Bronstein JM, Kachar B, Lazzarini RA. CNS myelin and sertoli cell tight junction strands are absent in Osp/claudin-11 null mice. Cell. 1999; 99(6):649–659. [PubMed: 10612400]

Graziano A, Liu XB, Murray KD, Jones EG. Vesicular glutamate transporters define two sets of glutamatergic afferents to the somatosensory thalamus and two thalamocortical projections in the mouse. J Comp Neurol. 2008; 507:1258–76. [PubMed: 18181146]

Honke K, Hirahara Y, Dupree J, Suzuki K, Popko B, Fukushima K, Fukushima J, Nagasawa T, Yoshida N, Wada Y, Taniguchi N. Paranodal junction formation and spermatogenesis require sulfoglycolipids. Proc Natl Acad Sci U S A. 2002; 99(7):4227–4232. [PubMed: 11917099]

Ishibashi T, Dupree JL, Ikenaka K, Hirahara Y, Honke K, Peles E, Popko B, Suzuki K, Nishino H, Baba H. A myelin galactolipid, sulfatide, is essential for maintenance of ion channels on myelinated axon but not essential for initial cluster formation. J Neurosci. 2002; 22(15):6507–6514. [PubMed: 12151530]

Jacobs EC. Genetic alterations in the mouse myelin basic proteins result in a range of dysmyelinating disorders. J Neurol Sci. 2005; 228(2):195–197. [PubMed: 15694204]

Jarjour AA, Bull SJ, Almasieh M, Rajasekharan S, Baker KA, Mui J, Antel JP, Di Polo A, Kennedy TE. Maintenance of axo-oligodendroglial paranodal junctions requires DCC and netrin-1. J Neurosci. 2008; 28(43):11003–11014. [PubMed: 18945908]

Marcus J, Honigbaum S, Shroff S, Honke K, Rosenbluth J, Dupree JL. Sulfatide is essential for the maintenance of CNS myelin and axon structure. Glia. 2006; 53(4):372–381. [PubMed: 16288467]

Mierzwa, A.; Arevalo, J.; Baigorri, B.; Campbell, K.; Chao, M.; Rosenbluth, J. A long-lived, spontaneous mouse mutation characterized by severe CNS dysmyelination. San Diego, CA: 2004.

Mierzwa, A.; Arevalo, J.; Chao, M.; Rosenbluth, J. Evidence for myelin instability in a shaking mouse mutant. Washington, DC: 2005.

Mierzwa, A.; Rosenbluth, J.; Lang, E. Evidence that CNS rather than PNS defects underlie the ‘shaking’ mouse phenotype. Washington DC: 2008.

Miotke JA, MacLennan AJ, Meyer RL. Immunohistochemical localization of CNTFRalpha in adult mouse retina and optic nerve following intraorbital nerve crush: evidence for the axonal loss of a trophic factor receptor after injury. J Comp Neurol. 2007; 500:384–400. [PubMed: 17111380]

Peles E, Nativ M, Lustig M, Grumet M, Schilling J, Martinez R, Plowman GD, Schlessinger J. Identification of a novel contactin-associated transmembrane receptor with multiple domains implicated in protein-protein interactions. EMBO J. 1997; 16:978–88. [PubMed: 9118959]

Pillai AM, Thaxton C, Pribisko AL, Cheng JG, Dupree JL, Bhat MA. Spatiotemporal ablation of myelinating glia-specific neurofascin (Nfasc(NF155)) in mice reveals gradual loss of paranodal

axoglial junctions and concomitantdisorganization of axonal domains. J Neurosci Res. 2009; 87(8):1773–1793. [PubMed: 19185024]

Poliak S, Gollan L, Martinez R, Custer A, Einheber S, Salzer JL, Trimmer JS, Shrager P, Peles E. Caspr2, a new member of the neurexin superfamily, is localized at the juxtaparanodes of myelinated axons and associates with K+ channels. Neuron. 1999; 1999–24:1037–47.

Rasband MN, Peles E, Trimmer JS, Levinson SR, Lux SE, Shrager P. Dependence of nodal sodium channel clustering on paranodal axoglial contact in the developing CNS. J Neurosci. 1999; 19:7516–28. [PubMed: 10460258]

Rios JC, Rubin M, St Martin M, Downey RT, Einheber S, Rosenbluth J, Rock Levinson S, Bhat M, Salzer L. Paranodal interactions regulate expression of sodium channel subtypes and provide a diffusion barrier for the node of Ranvier. J Neurosci. 2003; 23:7001–11. [PubMed: 12904461]

Rosenbluth J. Central myelin in the mouse mutant shiverer. J Comp Neurol. 1980; 194(3):639–648. [PubMed: 7451686]

Rosenbluth J. Axoglial junctions in the mouse mutant Shiverer. Brain Res. 1981; 208(2):283–297. [PubMed: 6163507]

Rosenbluth, J. Glial membranes and axonal junctions. In: Kettenmann, H.; Ransom, B., editors. Neuroglia. New York: Oxford University Press; 1995a.

Rosenbluth, J. Pathology of demyelinated and dysmyelinated axons. In: Waxman, S.; Kocsis, J.; Stys, P., editors. The Axon: Structure, Function, and Pathophysiology. New York, NY: Oxford University Press; 1995b. p. 391-411.

Rosenbluth J. Multiple functions of the paranodal junction of myelinated nerve fibers. J Neurosci Res. 2009

Rosenbluth J, Dupree JL, Popko B. Nodal sodium channel domain integrity depends on the conformation of the paranodal junction, not on the presence of transverse bands. Glia. 2003; 41(3): 318–325. [PubMed: 12528185]

Rosenbluth, J.; Mierzwa, A.; Arevalo, A.; Chao, M. Correlation between transverse bands and lifespan in dysmyelinated mice. Washington, D.C: 2008.

Samorajski T, Friede RL, Reimer PR. Hypomyelination in the quaking mouse. A model for the analysis of disturbed myelin formation. J Neuropathol Exp Neurol. 1970; 29(4):507–523. [PubMed: 5471919]

Schaeren-Wiemers N, Bonnet A, Erb M, Erne B, Bartsch U, Kern F, Mantei N, Sherman D, Suter U. The raft-associated protein MAL is required for maintenance of proper axon--glia interactions in the central nervous system. J Cell Biol. 2004; 166(5):731–742. [PubMed: 15337780]

Sherman DL, Brophy PJ. Mechanisms of axon ensheathment and myelin growth. Nat Rev Neurosci. 2005; 6(9):683–690. [PubMed: 16136172]

Sherman DL, Tait S, Melrose S, Johnson R, Zonta B, Court FA, Macklin WB, Meek S, Smith AJ, Cottrell DF, Brophy PJ. Neurofascins are required to establish axonal domains for saltatory conduction. Neuron. 2005; 48:737–742. [PubMed: 16337912]

Sidman RL, Dickie MM, Appel SH. Mutant Mice (Quaking and Jimpy) with Deficient Myelination in the Central Nervous System. Science. 1964; 144:309–311. [PubMed: 14169723]

Susuki K, Baba H, Tohyama K, Kanai K, Kuwabara S, Hirata K, Furukawa K, Furukawa K, Rasband MN, Yuki N. Gangliosides contribute to stability of paranodal junctions and ion channel clusters in myelinated nerve fibers. Glia. 2007; 55(7):746–757. [PubMed: 17352383]

Suzuki K, Zagoren JC. Quaking mouse: an ultrastructural study of the peripheral nerves. J Neurocytol. 1977; 6(1):71–84. [PubMed: 190360]

Yang JW, Vacher H, Park KS, Clark E, Trimmer JS. Trafficking-dependent phosphorylation of Kv1.2 regulates voltage gated potassium channel cell surface expression. Proc Nat Acad Si (US). 2007; 104:20055–60.

Yoshihara T, Shino A, Ishii T, Kawakami M. Ultrastructural and immunohistochemical study of salivary duct carcinoma of the parotid gland. Ultrastruct Pathol. 1994; 18:553–8. [PubMed: 7855929]

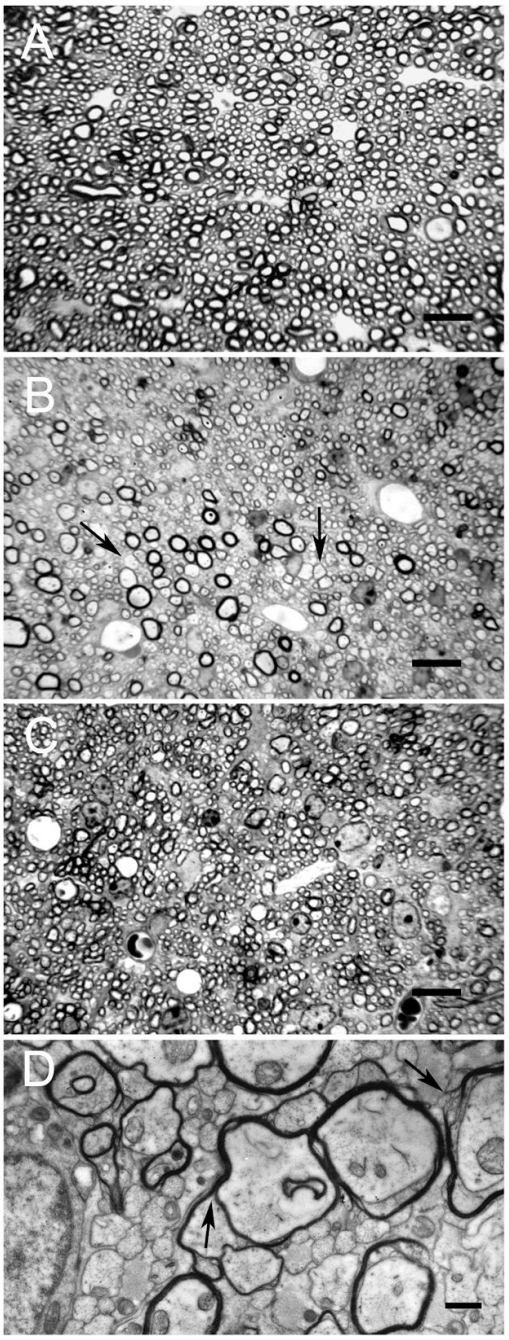

Figure 1.

A–C. Light micrographs of the dorsal columns in control (A), ‘shaking’ (B), and CST−/− (C) mice aged 6–9 months. Both ‘shaking’ and CST−/− display thin myelin sheaths (right arrow in B). Unmyelinated axons are abundant in ‘shaking’ (left arrow in B). Bar=10μ. D. Electron micrograph of ‘shaking’ optic nerve from 6 mo mouse showing unmyelinated and thinly myelinated axons as well as redundant myelin (left arrow) and cytoplasm-containing lamellae (right arrow). Bar=1μ.

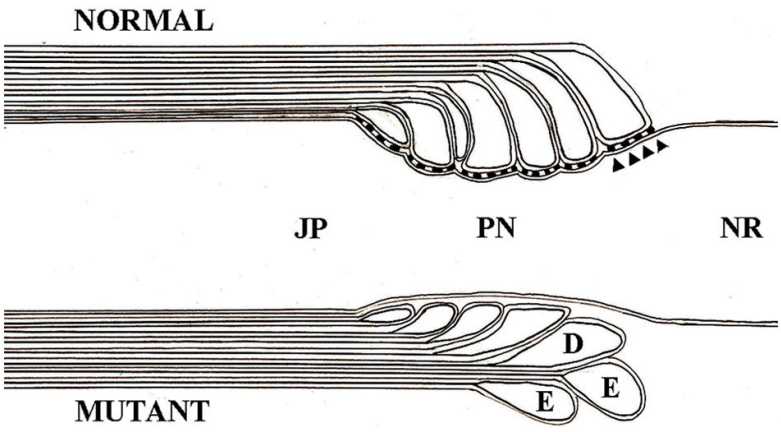

Figure 2.

Diagram showing a normal paranode (upper half) and a mutant paranode such as CST−/− (lower half). TBs are marked with arrowheads. NR= Node of Ranvier. PN= Paranode. JP= Juxtaparanode. D= Detached loop. E= Everted loops.

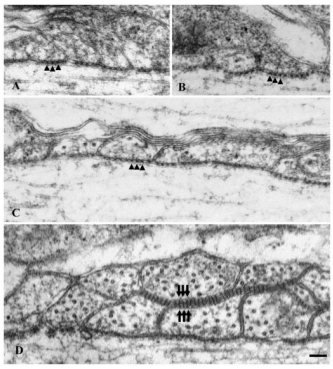

Figure 3.
Electron micrographs showing TBs in control (A) and ‘shaking’ (B, C) paranodes (arrowheads). The radial component (arrows) is very pronounced in ‘shaking’ paranodes (D). All pictures from 2.5mo animals. Bar=0.1μ.

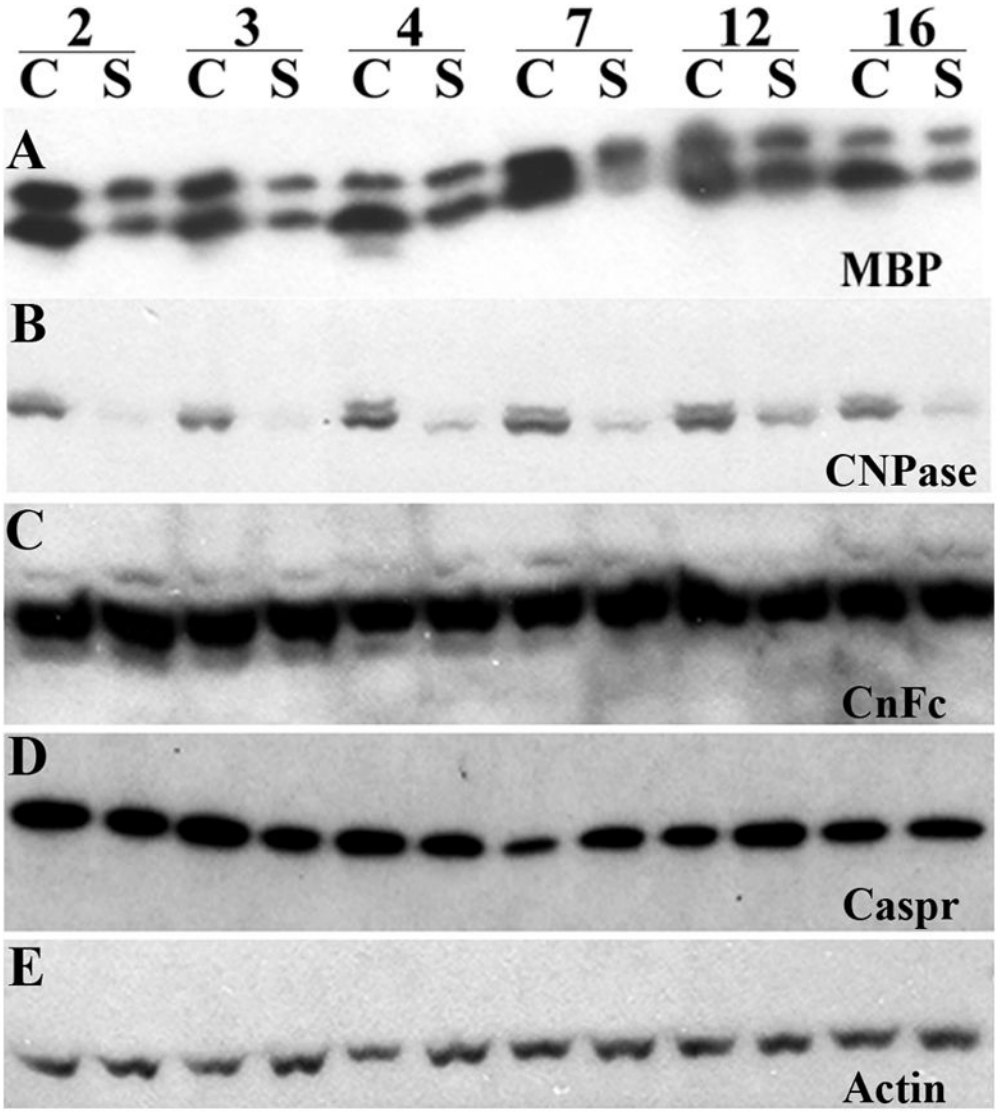

Figure 4.
Immunoblots of control (C) and shaking (S) brain specimens at different ages (2–16mo). MBP and CNPase levels are reduced in the shaking specimens at all ages. Contactin (CnFc) and Caspr levels are present at normal levels at all ages.

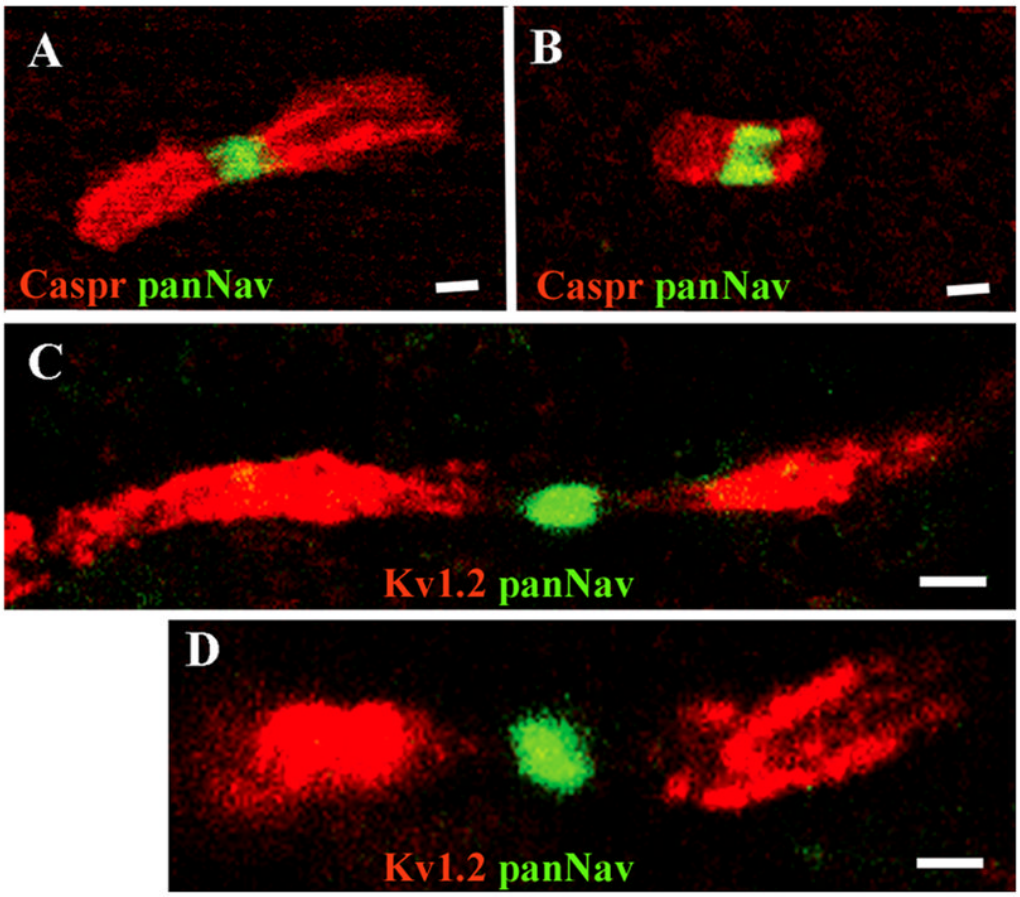

Figure 5.
Ion channel distribution in (A) control and (B) 'shaking' 7.5mo spinal cord. PanNav (green) and Caspr protein (red) are stained showing nodal and paranodal domains. Bar=1μ. (C) Control and (D) 'shaking' immunostaining in 6mo animals. PanNav (green) and $K_v1.2$ channels (red) are separated by an unstained paranode. (A magenta-green version is available as supplementary figure 1.)

Table 1

Details of antibodies used for immunostaining and western blots.

Antigen (what is being stained for)	Immunogen (what the antibody was raised against; full sequence and species)	Manufacturer, species antibody was raised in, mono- vs. polyclonal, catalog or lot number	Dilution used
MBP	Bovine myelin basic protein	Chemicon, Rat monoclonal antibody MAB386	1:500
CNPase	Full length native protein Human.	Roche Mouse monoclonal #1142007 clone 11-5B	1:1,000
CnFc	gel-purified F3 glycoprotein	Elior Peles' lab Mouse monoclonal antibodies	1:2,500
Caspr	GST fusion protein composed of the entire cytoplasmic domain (74 amino acids, Q1308 to E1381) of rat p190/Caspr (GST–190CT),	Elior Peles' lab. Rabbit polyclonal antibodies.	1:1,000 (WB) 1:200 (IHC)
Actin	A synthetic actin C-terminal peptide, Ser-Gly-Pro-Ser-Ile-Val-His-Arg-Lys-Cys-Phe, attached to Multiple Antigen Peptide (MAP) backbone	Sigma. Mouse monoclonal A-4700 AC-40 hybridoma	1:1,000
pan Nav	synthetic peptide CTEEQKKYYNAM KKLGSKK from the intracellular III–IV loop of Na^+ channel	Sigma. Mouse monoclonal S8809	1:200
Kv1.2	GST fusion protein with sequence YHRET EGEEQ AQYLQ VTSCP KIPSS PDLKK SRSAS TISKS DYMEI QEGVN NSNED FREEN LKTAN CTLAN TNYVN ITKML TDV, corresponding to residues 417–499 of rat Kv1.2 (Accession P15386).	Alomone labs. Rabbit polyclonal APC-010	1:200
Kv1.2	Fusion protein amino acids 428–499(cytoplasmic C-terminus) of rat Kv1.2 (accession number P63142), Epitope mapped to within amino acids 463–480	Neuromab Balb/C mouse monoclonal 75-008	1:200

Table 2

Myelin thickness and ion channel domains are altered in the ‘shaking’ mouse. G-ratio shows thinner myelin in the ‘shaking’ specimens. Ion channel domain lengths were measured on immunostained tissue (Fig. 5).

		Control	S.D.	‘Shaking’	S.D.	Significance
g-ratio	All ages	0.85	0.04	0.92	0.03	p<0.001
Nodal length	1 mo	0.61	0.25	1.16	0.66	p<0.001
	7.5 mo	0.65	0.23	0.89	0.34	p=0.003
Paranodal length	1 mo	2.32	1.02	1.33	0.69	p=0.002
	7.5mo	1.99	1.08	2.08	1.5	ns

Table 3

Paranodal structure. The percentage of paranodal loops that do not contact the axon but are not everted, the percentage of loops that do not contact the axon and are everted, and the percentage of paranodes with at least one TB were counted on electron micrographs of the paranode in control, CST−/−, and ‘shaking’ animals. The only significant differences found (**) were a reduction in the number of CST−/− paranodes with TBs as compared with normal and ‘shaking’ animals (both $p<0.001$).

Age/Animal		% not contacting axon	N	% everted loops	N	% w/transverse bands	N
6mo or younger	Control	12	6	9	6	**100**	12
	‘Shaking’	4	12	12	12	**93**	14
	CST−/−	4	8	10	8	**22**	9
Significance		ns		ns		**	
Over 6mo	Control	15	10	8	10	**100**	25
	‘Shaking’	7	19	7	19	**94**	18
	CST−/−	8	10	12	10	**14**	7
Significance		ns		ns		**	
All Ages	Control	14	16	11	16	**100**	36
	‘Shaking’	6	31	7	30	**94**	32
	CST−/−	11	18	15	19	**16**	19
Significance		ns		ns		**	

Table 4

Frequency of transverse bands. '% loops with TBs' is based on averages of counts from electron micrographs. '# TBs/micron' was calculated based on the number of transverse bands/micron of glial membrane length in only those paranodal loops that have transverse bands. 'Adjusted #TBs/micron' is based on the *total* number of paranodal loops that appose the axon (calculated as # TBs/micron X % loops with TBs/100). This approximates the number of transverse bands/micron in actual paranodes, including loops that do not have transverse bands as well as those that do.

	Control	S.D.	'Shaking'	S.D.	Significance
% loops with TBs	91		62		$p<0.01$
# TBs/micron	23.2	3.4	20.2	6.7	$p=0.04$
Adjusted # TBs/micron	21.1		12.5		--